1521-009X/44/5/720–731$25.00
Drug Metabolism and Disposition

http://dx.doi.org/10.1124/dmd.116.069419
Drug Metab Dispos 44:720–731, May 2016

Glycyrrhizin Protects against Acetaminophen-Induced Acute Liver Injury via Alleviating Tumor Necrosis Factor α–Mediated Apoptosis[S]

Tingting Yan, Hong Wang, Min Zhao, Tomoki Yagai, Yingying Chai, Kristopher W. Krausz, Cen Xie, Xuefang Cheng, Jun Zhang, Yuan Che, Feiyan Li, Yuzheng Wu, Chad N. Brocker, Frank J. Gonzalez, Guangji Wang, and Haiping Hao

State Key Laboratory of Natural Medicines, Key Laboratory of Drug Metabolism and Pharmacokinetics, China Pharmaceutical University, Nanjing, Jiangsu, People's Republic of China (Ti.Y., H.W., M.Z., Yi.C., X.C., J.Z., Yu.C., F.L., Y.W., G.W., H.H.); Laboratory of Metabolism, Center for Cancer Research, National Cancer Institute, National Institutes of Health, Bethesda, Maryland (Ti.Y., To.Y., K.W.K., C.X., C.N.B., F.J.G.)

Received January 13, 2016; accepted March 9, 2016

ABSTRACT

Acetaminophen (APAP) overdose is the leading cause of drug-induced acute liver failure in Western countries. Glycyrrhizin (GL), a potent hepatoprotective constituent extracted from the traditional Chinese medicine liquorice, has potential clinical use in treating APAP-induced liver failure. The present study determined the hepatoprotective effects and underlying mechanisms of action of GL and its active metabolite glycyrrhetinic acid (GA). Various administration routes and pharmacokinetics–pharmacodynamics analyses were used to differentiate the effects of GL and GA on APAP toxicity in mice. Mice deficient in cytochrome P450 2E1 enzyme (CYP2E1) or receptor interacting protein 3 (RIPK3) and their relative wild-type littermates were subjected to histologic and biochemical analyses to determine the potential mechanisms. Hepatocyte death mediated by tumor necrosis factor α (TNFα)/caspase was analyzed by use of human liver-derived LO2 cells. The pharmacokinetics–pharmacodynamics analysis using various administration routes revealed that GL but not GA potently attenuated APAP-induced liver injury. The protective effect of GL was found only with intraperitoneal and intravenous administration and not with gastric administration. CYP2E1-mediated metabolic activation and RIPK3-mediated necroptosis were unrelated to GL's protective effect. However, GL inhibited hepatocyte apoptosis via interference with TNFα-induced apoptotic hepatocyte death. These results demonstrate that GL rapidly attenuates APAP-induced liver injury by directly inhibiting TNFα-induced hepatocyte apoptosis. The protective effect against APAP-induced liver toxicity by GL in mice suggests the therapeutic potential of GL for the treatment of APAP overdose.

Introduction

Acetaminophen (APAP) overdose is a leading cause of drug-induced acute liver failure in the United States (Blieden et al., 2014). Because of its prevalence and severity, the U.S. Food and Drug Administration decided to limit and monitor the exposure of high-dose APAP (McCarthy, 2014; Mitka, 2014). Cytochromes P450 enzymes, including CYP2E1, CYP3A11, and CYP1A2, are mainly responsible for the metabolic activation of APAP into its toxic intermediate, *N*-acetyl-*p*-benzoquinone imine (NAPQI) (Lee et al., 1996; Manyike et al., 2000; Cheung et al., 2005). High NAPQI production depletes glutathione (GSH), produces NAPQI-protein adducts, triggers mitochondrial oxidative stress, and ultimately initiates hepatocellular apoptosis and/or necrosis with acute liver inflammation.

The therapeutic options for treating APAP hepatotoxicity are limited. The only clinical choice is administration of *N*-acetyl cysteine. However, it has a narrow therapeutic time window after the onset APAP overdosing, and thus new antidotes are warranted (Lancaster et al., 2015).

In recent years, studies have revealed that some traditional Chinese medicines (TCMs) have therapeutic effects, and TCMs are recognized as potential drugs for ameliorating liver (Zhang and Schuppan, 2014) and other diseases (Chan et al., 2015; Xiong, 2015; Zheng et al., 2015). Notably, glycyrrhizin (GL), also known as glycyrrhizic acid, is one of the most effective medicines extracted from the TCM liquorice for treating liver diseases. GL has potent hepatoprotective (Li et al., 2014b), anti-inflammatory (Honda et al., 2012; Fu et al., 2014; Kim et al., 2015), and neuroprotective effects (Ni et al., 2013; Barakat et al., 2014). GL has been formulated as a drug widely used for treating chronic liver diseases in Asian countries (Li et al., 2014b). Structurally,

This work was supported by the Intramural Research Program of the National Institutes of Health National Cancer Institute and China Scholarship Council [No. 201407060024] and the National Natural Science Foundation of China [No. 81430091, 81325025, and 81273586]. The authors declare no conflicts of interest.
dx.doi.org/10.1124/dmd.116.069419.
[S]This article has supplemental material available at dmd.aspetjournals.org.

ABBREVIATIONS: APAP, acetaminophen; CYP, cytochrome P450 enzymes; ALT, alanine aminotransferase; AST, aspartate aminotransferase; DMSO, dimethyl sulfoxide; FACS, fluorescence-activated cell sorting; GA, glycyrrhetinic acid; GA50, 50 mg/kg of GA; 18β-GA, 18β-glycyrrhetinic acid; GL, glycyrrhizin; GL50, 50 mg/kg of glycyrrhizin; GL100, 100 mg/kg of glycyrrhizin; GSH, glutathione; GSSG, glutathione disulfide; IL, interleukin; MTT, thiazolyl blue tetrazolium bromide; NAC-APAP, *N*-acetyl cysteinyl–acetaminophen; NAPQI, *N*-acetyl-*p*-benzoquinone; NAPQI-GSH, 3-glutathionyl-acetaminophen; MLKL, mixed lineage kinase domain-like protein; NEC-1, necrostatin-1; RIPK, receptor interacting protein kinase; TCM, traditional Chinese medicine; TNFα, tumor necrosis factor α; TNFR1, tumor necrosis factor α receptor 1; TUNEL, terminal deoxynucleotidyl transferase–mediated digoxigenin-deoxyuridine nick-end labeling; zVAD, ZVAD-fmk, *N*-benzyloxycarbonyl-Val-Ala-Asp(*O*-methyl)-fluoromethyl ketone.

GL is a glycoside that is rapidly hydrolyzed to glycyrrhetinic acid (GA) by intestinal bacteria (Akao et al., 1994; Takeda et al., 1996). In a previous study, single intraperitoneal injections of GL were used as an inhibitor of high-mobility group box-1 (HMGB1) to confirm its pathophysiologic role in APAP toxicity (Wang et al., 2013). Pretreatment with GL (400 mg/kg) for 7 consecutive days attenuated APAP-induced hepatotoxicity by reversing fatty acid metabolism (Yu et al., 2014). GL's hydrolyzed metabolite, GA, was demonstrated to directly protect against several types of liver injury induced by exposure to carbon tetrachloride (Jeong et al., 2002; Chen et al., 2013), free fatty acids (Wu et al., 2008), and toxic bile acids (Gumpricht et al., 2005). However, it remains unknown whether GL's hepatoprotective effect is derived from GL or its putative active metabolite GA, and how either protects against APAP-induced cell death of hepatocytes.

The type and mechanism of APAP-triggered death of hepatocytes are still topics of debate. The protein complex of receptor interacting protein kinase-1 (RIPK1) and RIPK3, also known as necrosome, performs necroptosis (Li et al., 2012). The RIPK1 inhibitor necrostatin-1 (NEC-1) and the RIPK3 inhibitor dabrafenib have been reported to protect against APAP-induced hepatotoxicity both in vivo and in vitro, suggesting that necroptosis plays a role in protection (Li et al., 2014a; Takemoto et al., 2014). Two studies used gene knockout mice to elucidate the roles of necrosome signaling genes, including *Ripk1*, *Ripk3*, and *Mlkl*, in mediating APAP-induced toxicity. However, these two studies reported different results about the role of RIPK3 in APAP-induced toxicity. One study showed that RIPK3 was an early mediator of APAP-induced toxicity (Ramachandran et al., 2013), and the other study showed no difference in sensitivity to APAP between *Ripk3*-null mice and their wild-type littermates (Dara et al., 2015). Thus, the role of RIPK3-mediated necroptosis in APAP-induced hepatocyte death remains controversial.

APAP induces a severe inflammatory response in the liver (Lawson et al., 2000) and significant GSH depletion (Matsumaru et al., 2003). Tumor necrosis factor-α (TNFα) potentiates apoptotic hepatocyte death under conditions of low cellular GSH (Colell et al., 1998; Matsumaru et al., 2003). These studies suggest possible synergy with proinflammatory cytokines in mediating hepatocyte damage. Some studies have suggested that GL prevents the release of proinflammatory cytokines from immune cells (Fu et al., 2014; Kim et al., 2015), making GL a potential immunoregulator. However, the crosstalk among TNFα, APAP, and the effects of GL on this process, especially in hepatocytes, is still poorly understood.

In this study, the hepatoprotective effects of GL and GA against APAP-induced hepatotoxicity were examined to uncover the potential mechanisms involved in the protective effects. The protective effect of GL on APAP-induced liver injury is not derived from the metabolic inhibition of APAP activation and is unlikely to be related to RIPK3/necroptosis. The intraperitoneal or intravenous injection of GL, but not the intraperitoneal injection of GA or the intragastric administration of GL, had a potent hepatoprotective effect via interference with TNFα-induced hepatocyte apoptosis.

Materials and Methods

Chemicals and Reagents. GL (97%) and GA (99.5%) were purchased from TCI (Shanghai, People's Republic of China). 18β-Glycyrrhetinic acid (18β-GA; 97%), APAP, NEC-1, ammonium diethyldithiocarbamate, ketoconazole, formic acid, dimethyl sulfoxide (DMSO), thiazolyl blue tetrazolium bromide (MTT), and chlorpropamide were purchased from Sigma-Aldrich (St. Louis, MO). Acetaminophen glutathione disodium salt (NAPQI-GSH) was purchased from Toronto Research Chemicals (Toronto, Ontario, Canada). *N*-acetyl cysteine–acetaminophen (NAC-APAP) standard was kindly provided by Professor Bernhard Lauterburg, University of Bern, Switzerland. Recombinant human TNFα was purchased from Peprotech (London, United Kingdom). *N*-benzyloxycarbonyl-Val-Ala-Asp(*O*-methyl)-fluoromethyl ketone (ZVAD-fmk; zVAD) and the GSH/glutathione disulfide (GSSG) assay kit were purchased from Beyotime Institute of Biotechnology (Jiangsu, People's Republic of China). High-performance liquid chromatography–grade methanol and acetonitrile were obtained from Merck (Damstadt, Germany). Deionized water was purified using a Milli-Q system (Millipore, Billerica, MA). Enzyme-linked immunosorbent assay kits for mouse TNFα were purchased from Excel (Shanghai, People's Republic of China). The annexin V fluorescein isothiocyanate apoptosis detection kit was purchased from BD Biosciences (San Diego, CA), and the fluorescence-activated cell sorting (FACS) analysis was performed on a BD Accuri C6 flow cytometer (BD Biosciences). The In Situ Cell Death Detection Kit, AP was purchased from Roche (Indianapolis, IN).

Experimental Animals and Treatments

Male C57BL/6 wild-type mice (6 to 8 weeks old) were obtained from the Shanghai SLAC Laboratory Animal Center (Shanghai, People's Republic of China) and allowed free access to food and water until experimental use. The animal room was maintained at 23 $\pm$ 1°C with a 12-hour light/dark cycle and 55% $\pm$ 5% humidity. The animal studies were approved by the animal ethics committee of China Pharmaceutical University and were performed in accordance with the *Guide for the Care and Use of Laboratory Animals* as adopted and promulgated by the U.S. National Institutes of Health.

Ripk3-null mice and wild-type mice on a C57BL/6N background were provided by Vishva Dixit (Genentech, South San Francisco, CA), and *Cyp2e1*-null mice on a 129/CV genetic background were maintained in the U.S. National Cancer Institute, with handling in accordance with animal study protocols approved by the National Cancer Institute Animal Care and Use Committee. Before intraperitoneal dosing of APAP, the mice were fasted overnight (14 hours) with free access to water.

Mice were administered 600 mg/kg of APAP for inducing hepatotoxicity in *Cyp2e1*-null mice, 300 mg/kg of APAP for inducing hepatotoxicity in wild-type C57BL/6 mice, and 200 mg/kg of APAP for inducing hepatotoxicity in wild-type 129/CV mice. For single GL/GA treatments, GL by intragastric administration was performed at 1 hour before APAP dosing, GL or GA treatment was administered by intraperitoneal injection at 30 minutes before APAP dosing, and GL treatment by intravenous injection was coadministrated with APAP dosing. A dose of 50 mg/kg or 100 mg/kg of GL (GL50 or GL100, respectively) and 50 mg/kg of GA (GA50) or 30 mg/kg of 18β-GA was injected to mice; the mice were killed at 0, 0.5, 2, 4, 6, 8, and 24 hours, and serum and livers were collected. For multiple GL injections, mice were pretreated with 50 mg/kg of GL for 7 consecutive days, subjected to APAP overdosing 30 minutes after final GL injection, and sacrificed at 24 hours after APAP challenge. A portion of liver was fixed in 10% formalin solution, and the remaining liver was flash frozen in liquid nitrogen and stored at −80°C for further use. APAP was freshly dissolved in warm saline at 55°C and cooled to 37°C before use. GL was freshly dissolved in saline with the pH adjusted to 7.0–7.2. GA or 18β-GA was freshly dissolved in saline containing 5% Tween 80.

In Vitro Studies. Human nontumor hepatic LO2 cells were obtained from the Chinese Academy of Sciences (Shanghai, People's Republic of China). For testing the protective effect of GL or GA against APAP-induced LO2 cell death, LO2 cells were seeded in 96-well plates for MTT assays or 6-well plates for FACS assays and then grown to 70%–90% confluence before use. GL, GA, or 18β-GA was dissolved in DMSO as stock solution and diluted 1000 times. APAP was dissolved in Dulbecco's modified Eagle's medium. LO2 cells were pretreated with control 0.1% DMSO, or GL, GA, or 18β-GA for 30 minutes before adding APAP. Only 0.1% DMSO-treated cells were set as the control group. For cell viability assays, MTT was added after 18 to 24 hours of APAP treatment. For FACS assays, samples were collected at 10 hours after APAP treatment and analyzed according to the instruction manual protocol for the annexin V fluorescein isothiocyanate apoptosis detection kit.

Serum Aminotransferase Analysis. Alanine aminotransferase (ALT) and aspartate aminotransferase (AST) were quantified using a standard clinical automatic analyzer or a commercial ALT or AST assay kit (Catachem, Bridgeport, CT).

Quantitative Real-Time Polymerase Chain Reaction. Total tissue RNA extraction was performed by using the RNAiso Plus reagent (Takara Biotechnology, Dalian, People's Republic of China) according to the manufacturer's

protocol. Purified total RNA was reverse-transcribed using the Prime Script RT Reagent Kit (Takara Biotechnology Co., Ltd.) according to the manufacturer's protocol. Quantitative real-time polymerase chain reaction was performed by using the ABI PRISM 7000 Sequence Detection System (Applied Biosystems, Bedford, MA) and SyBr Green reagent kit (Takara Biotechnology). Values were normalized to glyceraldehyde-3-phosphate dehydrogenase. Sequences for the primers are listed in Supplemental Table 1.

H&E Staining and Terminal Deoxynucleotidyl Transferase–Mediated Digoxigenin-Deoxyuridine Nick-End Labeling. Formalin-fixed liver tissues were embedded in paraffin and 5-μm-thick sections were cut for H&E staining and terminal deoxynucleotidyl transferase–mediated digoxigenin-deoxyuridine nick-end labeling (TUNEL) staining according to the manual protocols. Data represent $n = 3$ in each group for all the analyses.

Liquid Chromatography/Tandem Mass Spectrometry Analysis of GL and GA. Chromatographic separation was obtained on a Waters Acquity I Class UPLC system comprising a binary solvent manager, a flow-through needle autosampler, and column manager using a Waters Acquity BEH C-18 2.1 × 50 mm column. A liquid chromatography/tandem mass spectrometry method was used with multiple reaction monitoring in positive mode for monitoring 823.7→453.5 for GL, 471.5→149.1 for GA, and 277→110.9 for the internal standard chlorpropamide with a slight modification of the mobile phase, as previously described by Li et al. (2013).

Liquid Chromatography with Quadrupole Time of Flight Mass Spectrometry Analysis of NAPQI-GSH. The oxidized APAP intermediate NAPQI, formed in the mouse microsomal incubation system, was trapped by reduced GSH with a slight modification of the in vitro APAP incubation system as described elsewhere (Fan et al., 2014; Jiang et al., 2015). NAPQI-GSH was determined by the liquid chromatography with quadrupole time of flight mass spectrometry (Q-TOF LC/MS) method. Briefly, mouse liver microsomes (final concentration 1 mg/ml protein) were incubated with 500 μM APAP alone and with GL (10 μM, 50 μM, 100 μM, 200 μM, and 500 μM), or GA/18β-GA (2 μM, 5μM, 10 μM, and 20 μM). The reaction was initiated by adding NAPDH, trapped by 5 mM GSH and quenched by adding cold acetonitrile. NAPQI-GSH was identified through accurate mass measurement, compared with authentic standards, and monitored at m/z 457.1393. The internal standard chlorpropamide was monitored at m/z 277.0414 in positive mode. Chromatographic separation was obtained on a Waters Synapt-HDMS Q-TOF mass spectrometer running in positive electrospray ionization mode. The capillary and cone voltage were 3.0 kV and 30 V, respectively. The source and desolvation temperature were 150°C and 400°C. The desolvation and cone gas (nitrogen) were 850 l/h and 50 l/h. Sulfadimethoxine (100 pg/μl) was used for lock-spray mass and infused at 70 μl/min. The mobile phases were: A, water with 0.1% formic acid; and B, acetonitrile with 0.1% formic acid. The flow rate was maintained at 0.4 ml/min. The gradient was as follows: initial conditions 98% A for 0.5 minutes, to 80% A at 4 minutes, to 5% A at 8.0 minutes; held for 1 minute; and returning to initial conditions and holding for 2 minutes for column equilibration, with a total running time of 11 minutes.

Statistical Analysis. Data are presented as the mean ± S.E.M. Differences between the control and experimental groups were determined by a two-tailed Student's t test in GraphPad Prism 6 (GraphPad Software, San Diego, CA). $P < 0.05$ was considered statistically significant.

Results

Intraperitoneal Administration of GL Reduces APAP-Induced Hepatotoxicity. To determine whether GL attenuates APAP-mediated damage in vivo, a nonlethal dose of APAP (300 mg/kg) was administered to wild-type mice and serum liver enzyme levels and histology were measured to determine hepatocellular toxicity after 24 hours. Serum ALT and AST were sharply increased in the vehicle/APAP-treated group, and they were markedly decreased in the GL/APAP-treated group (Fig. 1, A and B). Necrotic areas were markedly decreased in liver from GL-treated mice (Fig. 1C). Because APAP-induced liver toxicity is associated with increased inflammation (Lawson et al., 2000; Liu et al., 2004), the APAP-induced inflammatory response was analyzed. Secreted TNFα in serum was assessed in the APAP-administrated mice treated with or without GL. Serum TNFα levels were significantly reduced by

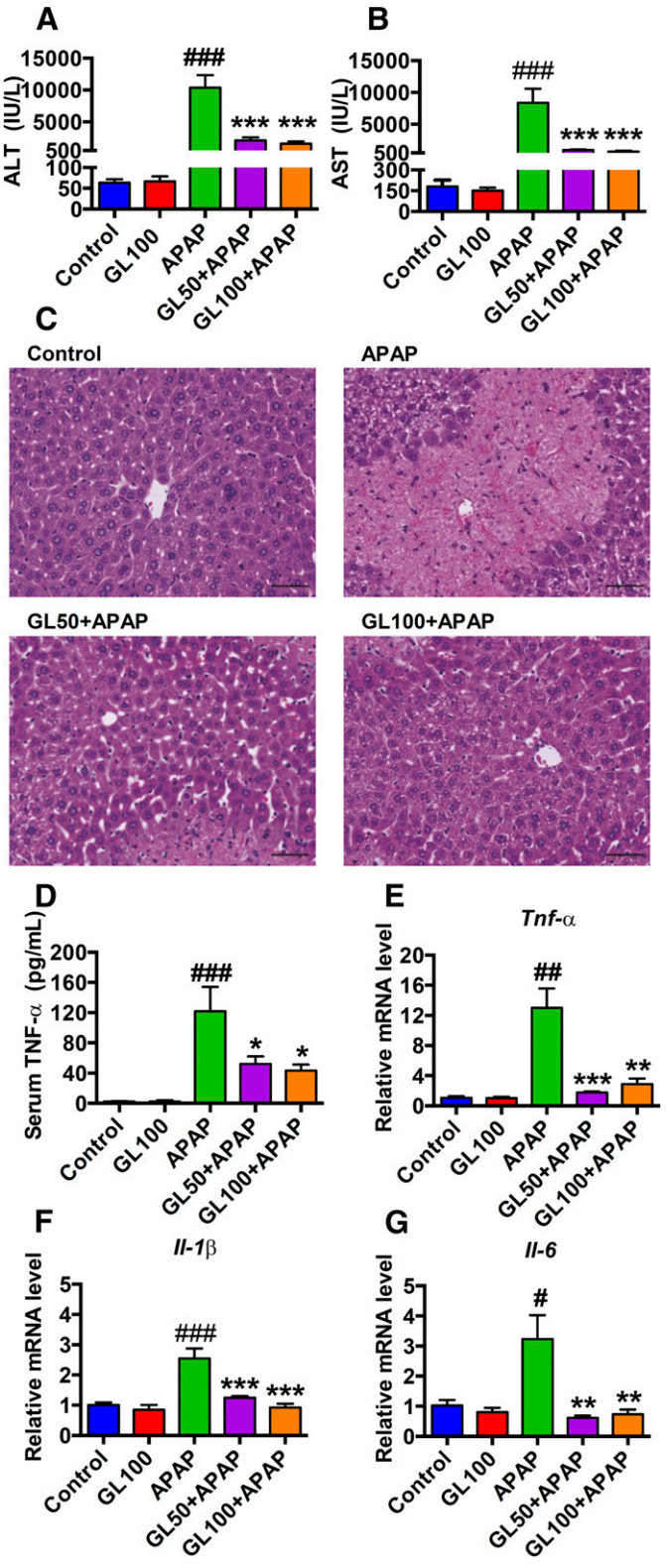

Fig. 1. GL pretreatment reduces serum transaminases, improves liver histology, and normalizes inflammation. (A, B) Serum ALT and AST levels. (C) H&E staining of liver sections. Original magnification, 20×; black scale bar, 50 μm. (D) Serum TNFα levels. (E–G), Relative mRNA level of TNFα, IL-1β, and IL-6 (n = 6–8 in each group). Control, saline-treated control mice; GL100, only GL 100 mg/kg-treated mice; APAP, saline/APAP-treated mice; GL50 + APAP, GL 50 mg/kg/APAP-treated mice; GL100 + APAP, GL 100 mg/kg/APAP-treated mice. Data are expressed as mean ± S.E.M. $^{\#}P < 0.05$, $^{\#\#}P < 0.01$, and $^{\#\#\#}P < 0.001$ versus control mice. $^{*}P < 0.05$, $^{**}P < 0.01$, and $^{***}P < 0.001$ versus APAP-overdosed mice.

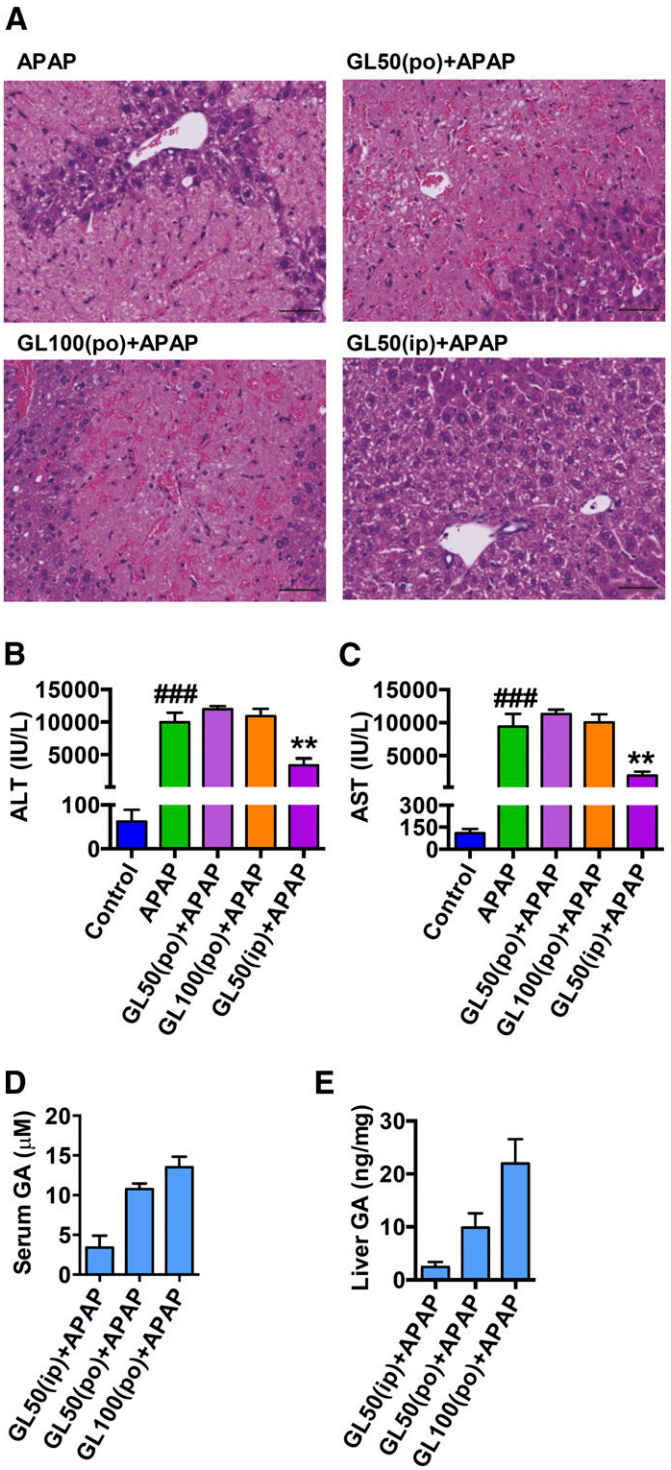

Fig. 2. Intragastric administration of GL fails to prevent APAP-induced hepatotoxicity. (A) H&E-stained liver sections 24 hours after APAP challenge. Original magnification, 20×; black scale bar, 50 μm. (B, C) Serum ALT and AST levels. (D, E) GL and GA levels in serum and liver. Control, saline-treated control mice; APAP, saline/APAP-treated mice; GL50 (po) + APAP, GL50 mg/kg (oral)/APAP-treated mice; GL100 (po) + APAP, GL100 mg/kg (oral)/APAP-treated mice; GL50 (ip) + APAP, GL50 mg/kg (i.p.)/APAP-treated mice. Data are expressed as mean ± S.E.M., n = 4–5 in each group. $^{###}P < 0.001$ versus control mice; $^{**}P < 0.01$ versus APAP-overdosed mice.

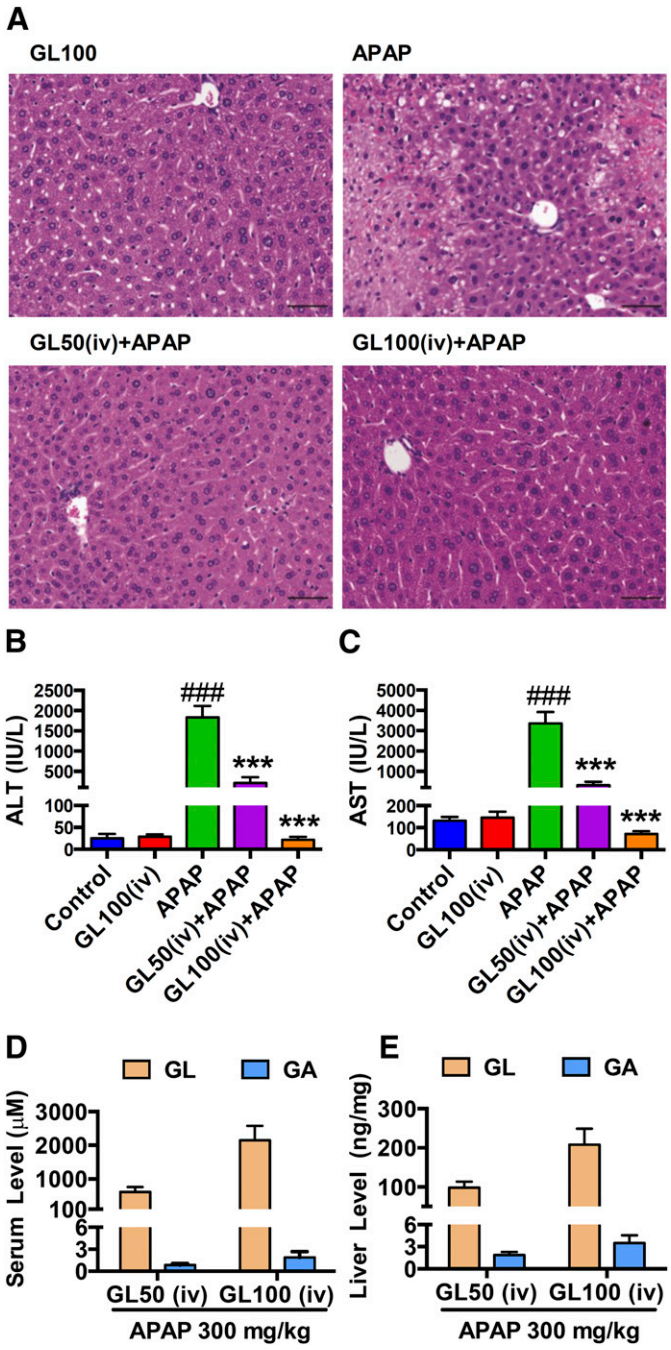

Fig. 3. Intravenous injection of GL inhibits APAP-induced hepatotoxicity. (A) H&E-stained liver sections 4 hours after APAP challenge. Original magnification, 20×; black scale bar, 50 μm. (B, C) Serum ALT and AST levels. (D, E) GL and GA levels in serum and liver. Data are expressed as mean ± S.E.M., n = 5–8 in each group for all analyses. Control, saline-treated control mice; APAP, saline/APAP-treated mice; GL50 (iv) + APAP, GL 50 mg/kg (i.v.)/APAP-treated mice; GL100 (iv) + APAP, GL 100 mg/kg (i.v.)/APAP-treated mice; GL100 (iv), only GL 100 mg/kg (i.v.)-treated mice. $^{###}P < 0.001$ versus control mice; $^{***}P < 0.001$ versus APAP-overdosed mice.

GL-treatment (Fig. 1D). Moreover, expression of mRNAs encoding the proinflammatory cytokines TNFα, interleukin 6 (IL-6), and IL-1β were normalized in the liver by pretreatment with GL (Fig. 1, E–G). Taken together, these results suggest that GL attenuated both liver toxicity and inflammation induced by APAP administration.

Intravenous, but Not Oral Administration of GL Inhibits APAP-Induced Hepatotoxicity. In the clinic, GL is administrated orally or intravenously, so we determined the effect of GL by intragastric administration or intravenous injection in APAP-caused liver injury. A single gavage administration of GL50 and GL100 showed no effect in

attenuating APAP-induced liver injury at 24 hours after APAP dosing (Fig. 2, A–C). GL was not detected, and GA was significantly detected in both serum and liver at 24 hours after APAP challenge (Fig. 2, D and E). GL50 by intraperitoneal injection was used as a positive control. Indeed, it is known that GL is hydrolyzed to GA by intestinal bacteria (Akao et al., 1994; Takeda et al., 1996). In contrast, intravenous injection of GL50 and GL100 decreased APAP-induced hepatocyte death (Fig. 3A) and markedly attenuated the increased serum ALT and AST levels (Fig. 3, B and C). By intravenous injection of GL50, the serum concentrations of GA were less than 1 μM in GL-alone injected mice and GL/APAP-treated mice, respectively, whereas approximately a 700-fold increase of GL was detected in the serum of GL/APAP-treated mice (Supplemental Fig. 1A and Fig. 3D). In the liver, the concentration of GA was 2 ng/mg, and a 50-fold increase of GL to approximately 100 ng/mg was detected (Supplemental Fig. 1B and Fig. 3E). Similarly, after intravenous administration of GL100, the serum and liver GA levels were markedly lower than GL levels (Fig. 3, D and E). These data indicate that GL attenuates liver injury only after intraperitoneal and intravenous administration and not gastric administration because GL was hydrolyzed in the gut into GA after oral administration.

GL, Not GA, Attenuates APAP-Induced Liver Damage. The observation that intravenous/intraperitoneal injection but not oral administration of GL showed a protective effect suggest that GL itself, and not the metabolite GA, directly contributed to GL's protective effect. To determine the compound responsible for GL's hepatoprotective effect, we investigated the pharmacokinetics and pharmacodynamics of injected GL after APAP dosing.

Mice were pretreated with a single intraperitoneal injection of GL100 30 minutes before APAP (300 mg/kg) challenge, and were killed at 2, 4, 8, and 24 hours after APAP (Fig. 4A). GL and GA distribution in liver and serum were then determined. During the time course of GL/APAP challenge, GL markedly attenuated APAP-caused liver injury. Intriguingly, the potent protective effect was observed even at the earliest time point of 2 hours, suggesting that GL could affect the initiation of APAP-induced toxicity and rapidly inhibit liver injury (Fig. 4, B and C). Moreover, GA levels peaked at 8 hours in liver and 4 hours in serum, while GL levels were time-dependently decreased in both serum and liver in GL/APAP-treated mice (Fig. 4, D and E) and in GL/saline-treated control mice (Supplemental Fig. 1, C and D).

Given that GA attenuates liver injury, ALT and AST would be expected to be decreased in a time-dependent manner. However, ALT and AST were markedly increased from 8 hours after APAP administration in the GL/APAP challenged group (Fig. 4, B and C). The potent protective effect of GL and increase in liver damage commencing at 8 hours were also confirmed by histology (Supplemental Fig. 1E). These data suggested that GL, and not GA, directly attenuated APAP hepatotoxicity.

To examine the direct effect of GA in combating APAP-induced liver injury, GA50 (approximately equimolar to GL100) was injected to wild-type mice by a single intraperitoneal injection before APAP (300 mg/kg) challenge. All mice were killed at 24 hours after APAP

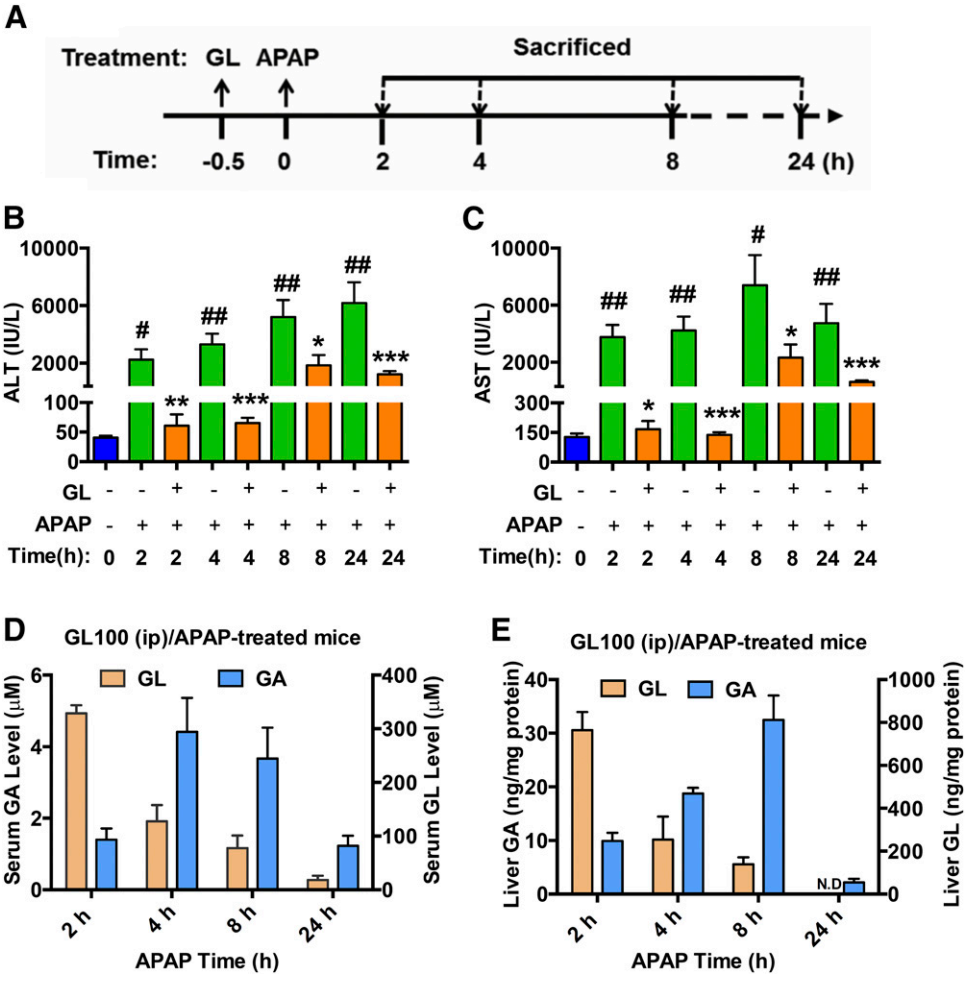

Fig. 4. Intraperitoneal injection of GL decreases serum ALT and AST level at the early stage after APAP challenge. (A) Mouse experiment procedure scheme. (B, C) Time course of serum ALT and AST levels after APAP challenge. (D, E) Pharmacokinetic distribution of GL and GA in serum (D) and liver (E) in GL100 (ip)/APAP-treated mice. Data are expressed as mean ± S.E.M., $n = 3$ in each group for control mice and $n = 6$ for other groups. $^{\#}P < 0.05$ and $^{\#\#}P < 0.01$ versus control mice. $^{*}P < 0.05$, $^{**}P < 0.01$, and $^{***}P < 0.001$ versus APAP-overdosed mice.

administration and subjected to histologic and serum analysis. In serum, GA was only detected in GA-treated mice and not detected in the GL-treated mice (Fig. 5A). In the liver, approximately a 10-fold increase of GA was detected in GA-treated mice compared with GL-treated mice (Fig. 5B). Thus, GA was efficiently absorbed and detected in both serum and liver. Histology revealed that the necrotic areas that developed after APAP in the GA-treated group were not decreased as compared with the nontreated group, while the areas were significantly decreased in the GL-treated group (Supplemental Fig. 2A).

In agreement with this result, ALT and AST were also decreased in the GL/APAP-treated group. In contrast, these markers in the GA-treated group were moderately but not significantly decreased (Fig. 5, C and D). Furthermore, the effect of 18β-GA showed no significant effect in preventing APAP-induced liver injury (Supplemental Fig. 2, B–D) whereas 18β-GA was efficiently absorbed in both serum and liver (Supplemental Fig. 2, E and F). These data demonstrate that the effects of GA derived from hydrolyzed GL in the GL-treated group in vivo could be excluded.

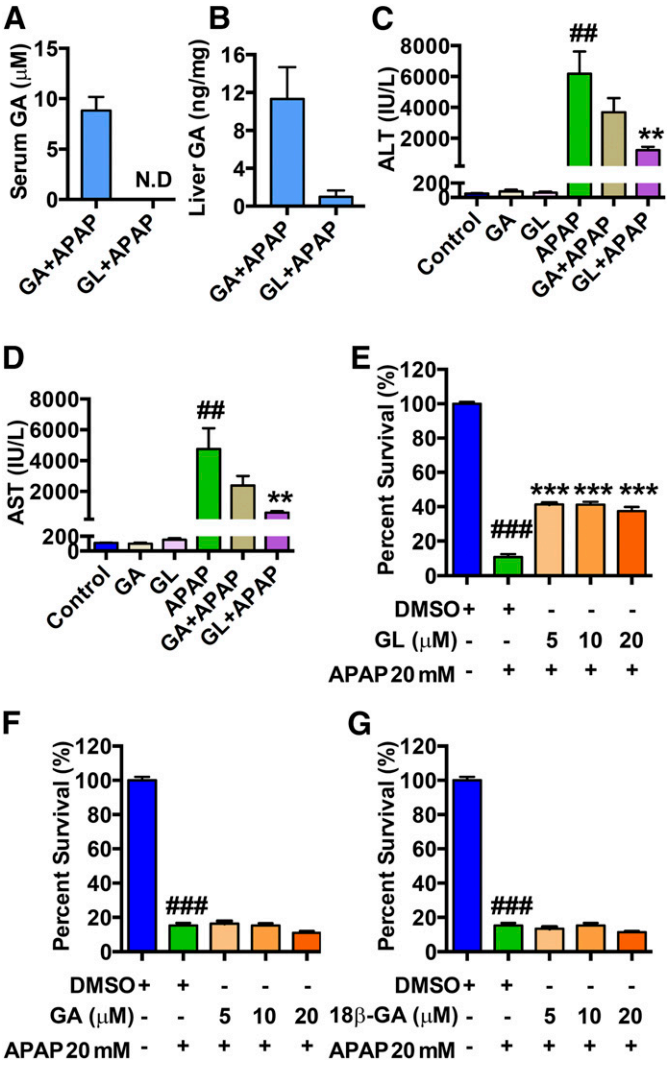

Fig. 5. GL, rather than GA, prevents APAP-induced hepatocyte damage both in APAP-overdosed mice and APAP-treated LO2 cells. (A, B) GA exposure in serum (A) and in liver (B) in GA/APAP-treated mice and GL/APAP-treated mice. (C, D) Serum ALT and AST levels. (E) Cell viability of GL/APAP 20 mM-treated LO2 cells. (F) Cell viability of GA/APAP 20 mM-treated LO2 cells. (G) Cell viability of 18β-GA/APAP 20 mM-treated LO2 cells. Data are expressed as mean ± S.E.M., n = 5–6 for both animal experiments and LO2 cell experiments. Control, saline-treated mice; GA, only GA 50 mg/kg-treated mice; GL, only GL 50 mg/kg-treated mice; APAP, saline/APAP-treated mice; GA + APAP, GA 50 mg/kg/APAP-treated mice; GL + APAP, GL 50 mg/kg/APAP-treated mice; $^{\#\#}P < 0.01$ and $^{\#\#\#}P < 0.001$ versus control mice or 0.1% DMSO-treated control LO2 cells. $^{**}P < 0.01$ and $^{***}P < 0.001$ versus APAP-overdosed mice or 0.1% DMSO/APAP-treated LO2 cells.

The direct effect of GL and the hydrolyzed form GA were next analyzed in vitro by use of human hepatic-derived LO2 cells. Cell survival rates were determined after APAP treatment together with GL, GA, or 18β-GA. GL was found to significantly inhibit APAP-induced cell death in vitro (Supplemental Fig. 3A) whereas neither GA nor 18β-GA showed protective potency against cytotoxicity induced by APAP (10 mM) (Supplemental Fig. 3, B and C). This protective effect was more remarkable at a higher dose of APAP (20 mM). GL significantly rescued the survival rate of APAP-treated cells from approximately 10% to 40%, even at the low concentration of 5 μM (Fig. 5E) whereas both GA and 18β-GA showed no significant protective effect at various concentrations (Fig. 5, F and G). Both concentrations of GA and 18β-GA used included the maximum nontoxic concentration in the hepatic cells (Supplemental Fig. 3, D–F). These data demonstrate that GL and not GA directly prevents APAP-caused liver injury by inhibiting hepatocyte damage.

Hepatoprotective Effect of GL Is Unrelated to the Metabolic Activation of APAP. To clarify the possible mechanisms, we first asked whether the hepatoprotective effect of GL against APAP toxicity was from the direct interference of APAP metabolic activation. We found that treatment with a single or multiple injections of GL alone to mice had no significant effect on the expression of *Cyp2e1*, *Cyp3a11*, or *Cyp1a2*, although both treatments significantly attenuated APAP-induced down-regulation of such enzymes (Fig. 6, A–C). Similar results were obtained from the in vitro mouse primary hepatocytes study; no significant change in the *Cyp2e1*, *Cyp3a11,* or *Cyp1a2* mRNA levels was observed with GL, GA, or 18β-GA (Supplemental Fig. 4, A–F).

APAP hepatotoxicity is mainly induced by NAPQI, which subsequently binds with hepatic GSH and forms NAPQI-GSH. To test whether GL and/or GA directly inhibited APAP bioactivation, an APAP/mouse liver microsome incubation system was used. A peak at the same retention time (1.9 minutes) with NAPQI-GSH authentic standard was found in the in vitro APAP incubation system whereas no peak was found when we removed NAPDH from the APAP incubation system (Supplemental Fig. 5A). In this system, we found that GL, GA, and 18β-GA did not significantly influence APAP metabolic activation in vitro whereas the positive CYP3A11 inhibitor (ketoconazole) and CYP2E1 inhibitor (ammonium diethyldithiocarbamate) significantly inhibited the formation of NAPQI-GSH (Fig. 6, D–F).

In mice, the hepatotoxic NAPQI produced from APAP metabolic activation is very unstable and has been known to subsequently form NAPQI-GSH and NAC-APAP (Chen et al., 2008). While we were determining the extent of APAP metabolic activation in vivo, we found that the serum level of NAPQI-GSH and NAC-APAP at 3 hours after APAP injection were not significantly changed by either a single GL injection or multiple GL injections (Fig. 6, G–H). Meanwhile, we analyzed the GSH/GSSG ratio in APAP-administrated and GL-treated liver. In time course experiments, 300 mg/kg of APAP administration resulted in a rapid depletion of GSH in the liver at 2 and 4 hours after administration; GL pretreatment did not alter the liver GSH/GSSG ratios at either time point (Supplemental Fig. 5B).

CYP2E1 has a significant role in the metabolic activation of APAP, as *Cyp2e1*-null mice show resistance to APAP toxicity (Lee et al., 1996). Analysis of the relationships between the protective effect of GL and CYP2E1-mediated APAP activation revealed that 200 mg/kg of APAP administered to wild-type129/CV mice or a

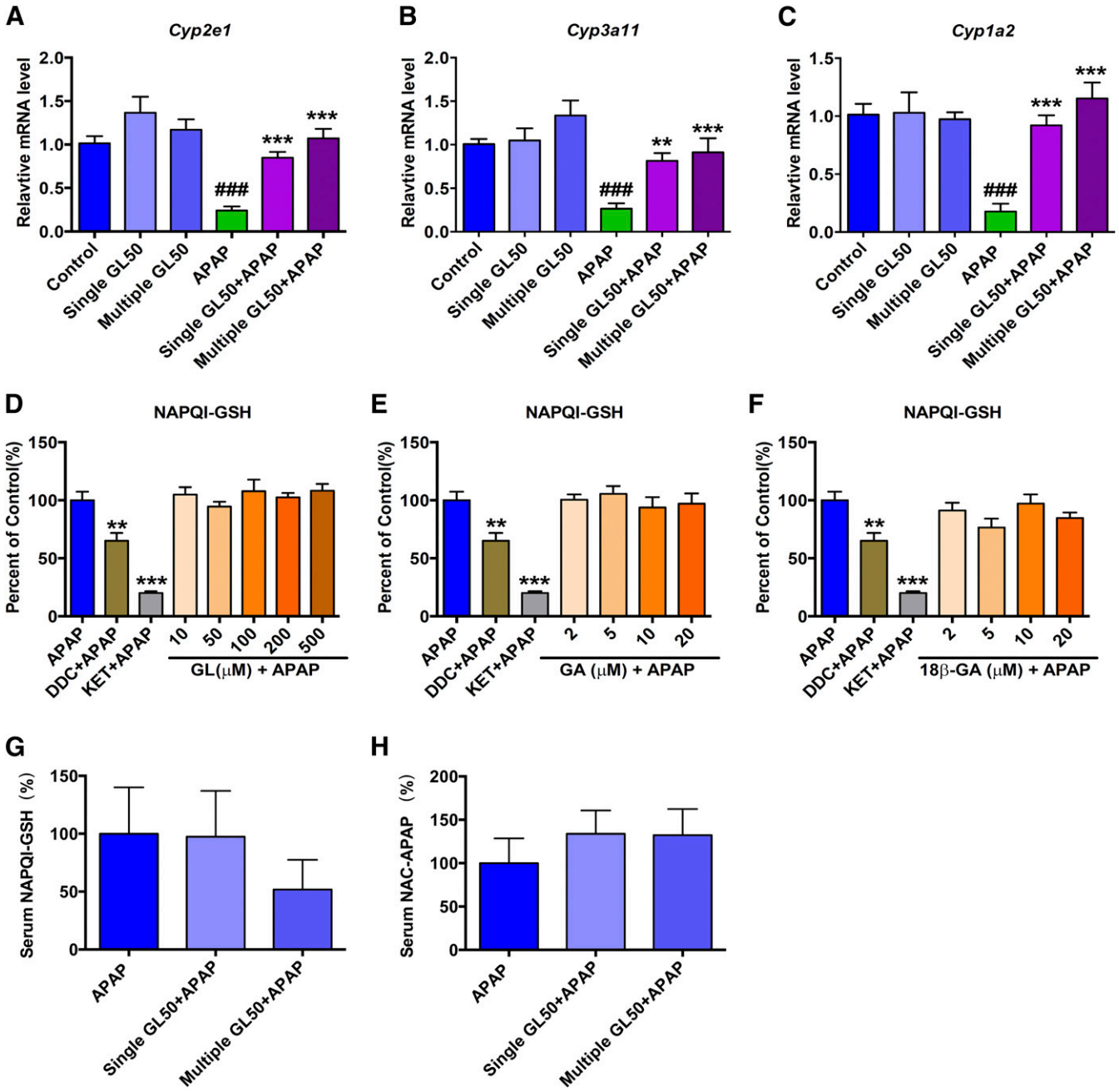

Fig. 6. GL shows no significant effect in mRNA level of *Cyp2e1*, *Cyp3a11*, or *Cyp1a2* or modifying APAP metabolic activation. (A–C) Effect of GL and/or APAP injection in the mRNA level of *Cyp2e1* (A), *Cyp3a11* (B), and *Cyp1a2* (C). (D–F) Effects of GL (D), GA (E), and 18β-GA (F) in production of NAPQI-GSH in APAP/mouse liver microsome incubation system. Serum NAPQI-GSH (G) and NAC-APAP (H) level. Control, saline-treated mice; Single GL50, only single GL 50 mg/kg-treated mice; APAP, saline/APAP-treated mice; Single GL50 + APAP, single injection of GL 50 mg/kg (i.p.)/APAP-treated mice. Multiple GL50 + APAP, multiple injections of GL 50 mg/kg (i.p.)/APAP-treated mice. DCC, ammonium diethyldithiocarbamate; KET, ketoconazole. Data are expressed as the mean ± S.E.M., $n = 5$ mice in each group. $^{\#}P < 0.05$, $^{\#\#}P < 0.01$, and $^{\#\#\#}P < 0.001$ versus control mice. $^{*}P < 0.05$, $^{**}P < 0.01$, and $^{***}P < 0.001$ versus APAP-overdosed mice.

high dose (600 mg/kg) of APAP administered to *Cyp2e1*-null mice induced liver injury, as revealed by the increased serum ALT and AST as well as severe hepatocytes death. In contrast, the injury markers were robustly inhibited by intraperitoneal injection of GL50 both 6 hours and 24 hours after APAP challenge in both wild-type (Fig. 7, A and B) and *Cyp2e1*-null mice (Fig. 7, C and D). Histology showed a similar attenuation of APAP-induced toxicity by GL in wild-type (Supplemental Fig. 6A) and *Cyp2e1*-null mice (Supplemental Fig. 6B). These results revealed that GL's protective effect did not depend on the metabolic activation of APAP and CYP2E1 expression. Together, these results strongly support that the hepatoprotective effect of GL is unrelated to the metabolic activation of APAP.

RIPK3 Is Not Involved in APAP Toxicity or the Hepatoprotective Effect of GL. Recent studies revealed a type of necrosis involved in programmed cell death known as necroptosis (Li et al., 2012). RIPK1 and RIPK3 are both central players in TNFα-induced necroptosis (Zhang et al., 2009; Li et al., 2012), with the involvement of its downstream cellular signaling mixed lineage kinase domain-like protein (MLKL) (Sun et al., 2012; Zhao et al., 2012). In

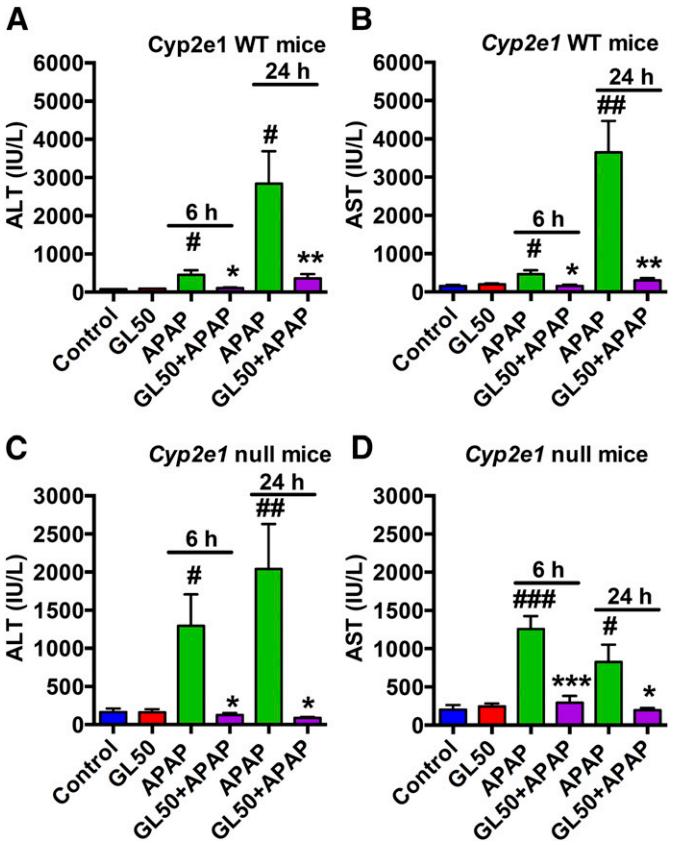

Fig. 7. GL markedly attenuates serum ALT and AST levels in both wild-type and *Cyp2e1*-null mice. (A, B) Serum ALT and AST levels in wild-type mice. (C, D) Serum ALT and AST levels in *Cyp2e1* null mice. Control, saline-treated mice; GL 50, only GL 50 mg/kg-treated mice; APAP, saline/APAP-treated mice; GL50 + APAP, GL 50 mg/kg (i.p.)/APAP-treated mice. WT, wild-type. Data are expressed as mean ± S.E.M., $n = 5$ mice in each group. $^{\#}P < 0.05$, $^{\#\#}P < 0.01$, and $^{\#\#\#}P < 0.001$ versus control mice. $^{*}P < 0.05$, $^{**}P < 0.01$, and $^{***}P < 0.001$ versus APAP-overdosed mice.

particular, RIPK3 was confirmed to have an essential role in ameliorating APAP-induced liver injury (Ramachandran et al., 2013). To confirm whether APAP exposure influenced RIPK3 expression, we measured *Ripk3* mRNA levels.

APAP induced a 2- to 3-fold increase of *Ripk3* mRNA as early as 2 hours (Supplemental Fig. 7A). Upstream signaling of RIPK3, *Tnfα*, and downstream *Mlkl* mRNA were also elevated (Supplemental Fig. 7, B and C). GL-treatment significantly attenuated both of the *Ripk3* and *Tnfα* mRNA levels whereas no significant decrease of *Mlkl* mRNA by GL treatment was noted (Supplemental Fig. 7, A–E). These results suggest that RIPK3-mediated necroptosis is possibly involved in APAP toxicity and GL's protective effect.

We further investigated with the use of *Ripk3*-null mice. The histologic observations (Fig. 8, A and B) and levels of serum ALT and AST (Fig. 8, C and D) showed no differences when we compared *Ripk3*-null mice and their wild-type littermates at 6 hours after APAP challenge. Furthermore, GL robustly and significantly attenuated APAP toxicity in both genotypes. These results suggested no involvement of RIPK3 in APAP-induced liver toxicity and that GL's protective effect against APAP toxicity was not through RIPK3/necroptosis. Conversely, these data suggest that RIPK3 up-regulation is possibly only a consequence, that RIPK3-mediated necroptosis is not a mediator of APAP-induced hepatocyte death, and that GL's protective effect does not depend on RIPK3.

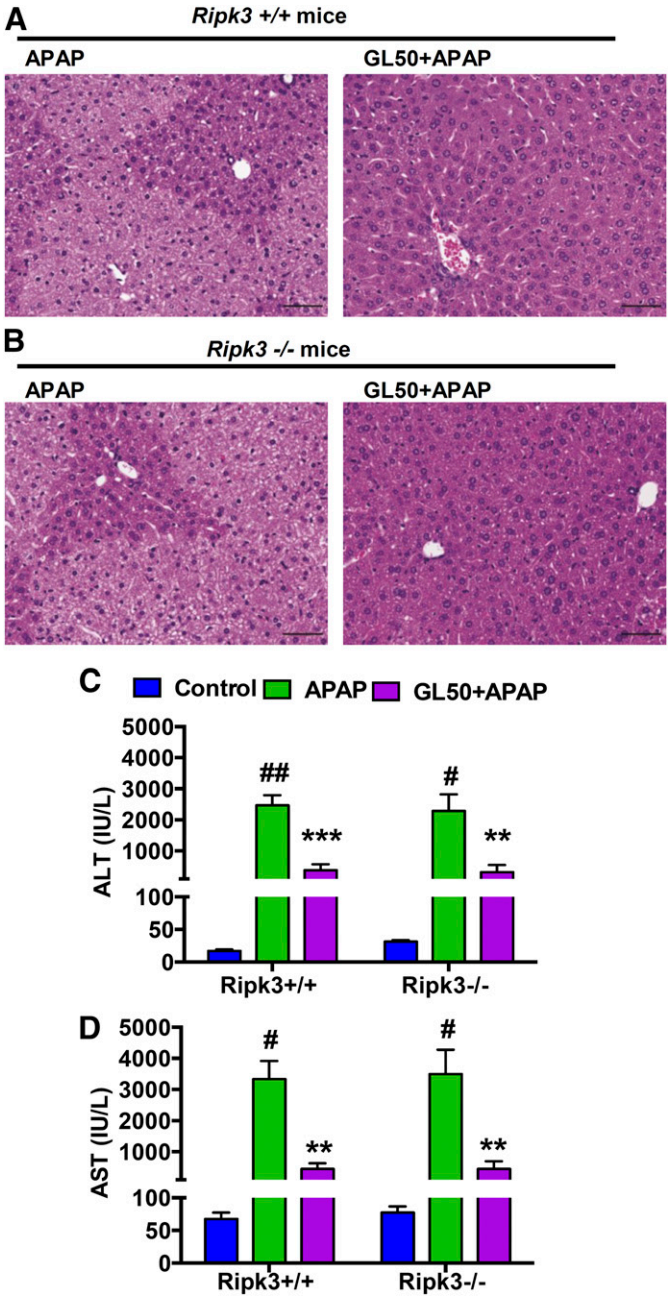

Fig. 8. GL combats APAP-induced hepatotoxicity in both *Ripk3*-null mice and their wild-type littermates. (A, B) H&E-stained liver sections of (A) $Ripk3^{+/+}$ mice and (B) $Ripk3^{-/-}$ mice. Original magnification, 20×; black scale bar, 50 μm. (C, D) Serum ALT and AST levels. Data are expressed as mean ± S.E.M., $n = 5$–6 mice for APAP and GL + APAP group and $n = 3$ for control group. Control, saline-treated control mice; APAP, saline/APAP-treated mice; GL50 + APAP, GL 50 mg/kg (i.p.)/APAP-treated mice. All experiments in *Ripk3*-null mice and their wild-type littermates were repeated twice. $^{\#}P < 0.05$; $^{\#\#}P < 0.01$ and $^{\#\#\#}P < 0.001$ versus control mice. $^{*}P < 0.05$, $^{**}P < 0.01$ and $^{***}P < 0.001$ versus APAP-overdosed mice.

GL Protects against TNFα-Mediated Apoptotic Hepatocyte Death. Because RIPK3-mediated necroptosis was demonstrated as unlikely to be a major player in APAP-induced liver injury, as noted in our data as well as in another recent publication (Dara et al., 2015), we investigated the possible role of apoptotic hepatocyte death and its extent with the use of the TUNEL assay. Mouse livers exposed to APAP revealed that TUNEL-positive cells emerged at the early phase (2 hours) after APAP dosing whereas few TUNEL-positive cells were

observed in GL/APAP-treated mice during the time course of the APAP challenge (Fig. 9). Analysis of mRNA encoding BCL2a1c, which is an apoptosis marker, also showed a 2- to 3-fold increase in APAP-challenged livers whereas the GL-treated groups showed a significant decrease in expression (Supplemental Fig. 7F).

The factors that initiate apoptotic hepatocyte death after APAP challenge remain largely unknown. TNFα, one of the apoptosis-inducible factors (Colell et al., 1998; Matsumaru et al., 2003), may mediate APAP-induced hepatocyte death. In vivo, APAP-administration induced significant TNFα release in serum as early as 2 hours after administration (Fig. 10A). GL100 treatment markedly decreased TNFα secretion at 4 hours after APAP injection (Fig. 10B).

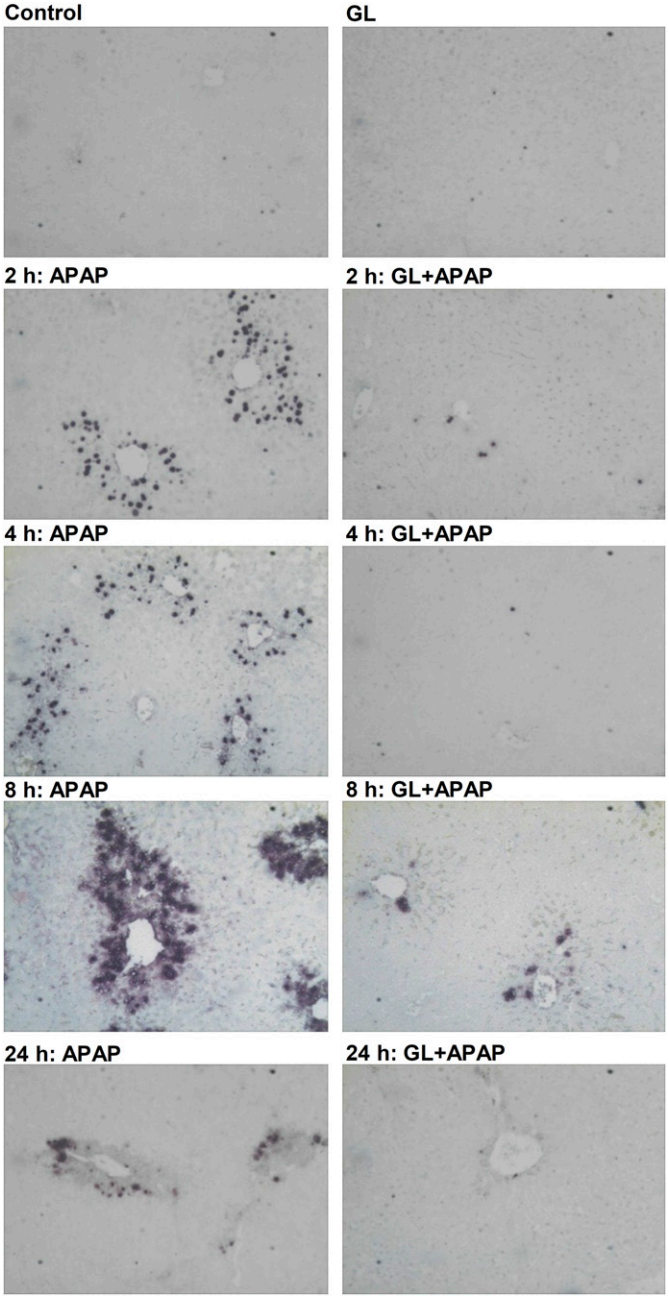

Fig. 9. GL blocks TUNEL-positive staining at the early stage after APAP challenge. TUNEL-staining analysis of paraffin-embedded livers. Original magnification, 20×. Control, saline-treated mice; GL, only GL 100 mg/kg-treated mice; APAP, saline/APAP-treated mice; GL + APAP, GL 100 mg/kg/APAP-treated mice.

Considering that the time course of TNFα release coincides well with that of the APAP toxicity, the involvement of TNFα in potentiating APAP-induced hepatocyte apoptosis needs to be considered. To validate this assumption, we tested the potentially synergistic role of TNFα with APAP toxicity in vitro. TNFα aggravated APAP-induced cytotoxicity in a dose-dependent manner in LO2 cells, although TNFα alone showed no significant effect on the cell viability (Fig. 10C). Interestingly, the pan-caspases inhibitor zVAD, but not the small necrosis inhibitor NEC-1, significantly inhibited TNFα/APAP-induced cytotoxicity (Fig. 10, C and D). The protective effect of zVAD was also observed in APAP-induced cytotoxicity (Fig. 10E). These results indicate that caspases-dependent apoptosis is a critical factor in both APAP and TNFα/APAP-induced cytotoxicity.

Furthermore, addition of GL, GA, or 18β-GA to the culture medium revealed that GL (Fig. 10D and Supplemental Fig. 3G) but not GA or 18β-GA (Supplemental Fig. 3, H and I) attenuated TNFα/APAP-induced cell death. FACS analysis further indicated that, although TNFα (20 ng/ml) alone did not induce apoptosis, TNFα/APAP markedly induced apoptotic cell death. In addition, apoptosis was potently inhibited by GL addition (Fig. 10F). These data demonstrate that GL, but not GA, attenuated APAP-induced hepatocyte damage via inhibiting the release of TNFα and its downstream caspase-dependent apoptotic signaling.

Discussion

In this study, GL, but not its active metabolite GA, was found to prevent APAP-induced liver injury via inhibiting TNFα/caspase-mediated apoptotic hepatocyte death. The hepatoprotective effect of GL was unlikely to be from the direct interference of APAP metabolic activation or through RIPK3-mediated necroptosis. Intraperitoneal or intravenous injection of GL, but not oral administration, had a potent protective effect against APAP-induced liver toxicity. Moreover, with GL as a chemical probe, this study revealed that the release of TNFα upon APAP challenge might be an important factor in APAP-induced hepatotoxicity via potentiating APAP-induced apoptotic cell death of hepatocytes.

One of the major challenges in ascertaining the hepatoprotective effects of GL is how to differentiate the role of GL and its bioactive metabolite GA. It is widely claimed that the hepatoprotective effect of GL is due to its metabolite GA; GL is rapidly metabolized to GA by the gut bacteria, so GL was previously assumed to be a prodrug. However, in the present study, evidence is provided that GL itself and not its bioactive metabolite GA contributes to the hepatoprotective effect against APAP toxicity. The transformation of GL to GA mainly happens in the intestine, so examining the differential effects of GL via different routes of administration would be helpful for differentiating the roles of GL and GA.

First, we found, unexpectedly, that intravenous or intraperitoneal injection of GL, but not intragastric administration, exerted a significantly protective effect. Second, a pharmacokinetics–pharmacodynamics correlation analysis demonstrated that GL, rather than GA, contributes to the hepatoprotective effect of GL, proving the potential application of "reverse pharmacokinetics" in the mechanistic studies of natural compounds (Hao et al., 2014). Finally, in vitro studies further revealed that GL, rather than GA, protected against APAP-induced hepatocyte damage. All these data strongly suggest that GL and not its metabolite GA possesses hepatoprotective activity against APAP-induced liver injury.

Given that GA shows a potent protective effect in liver injury caused by other toxicants, including carbon tetrachloride, bile acids, and free

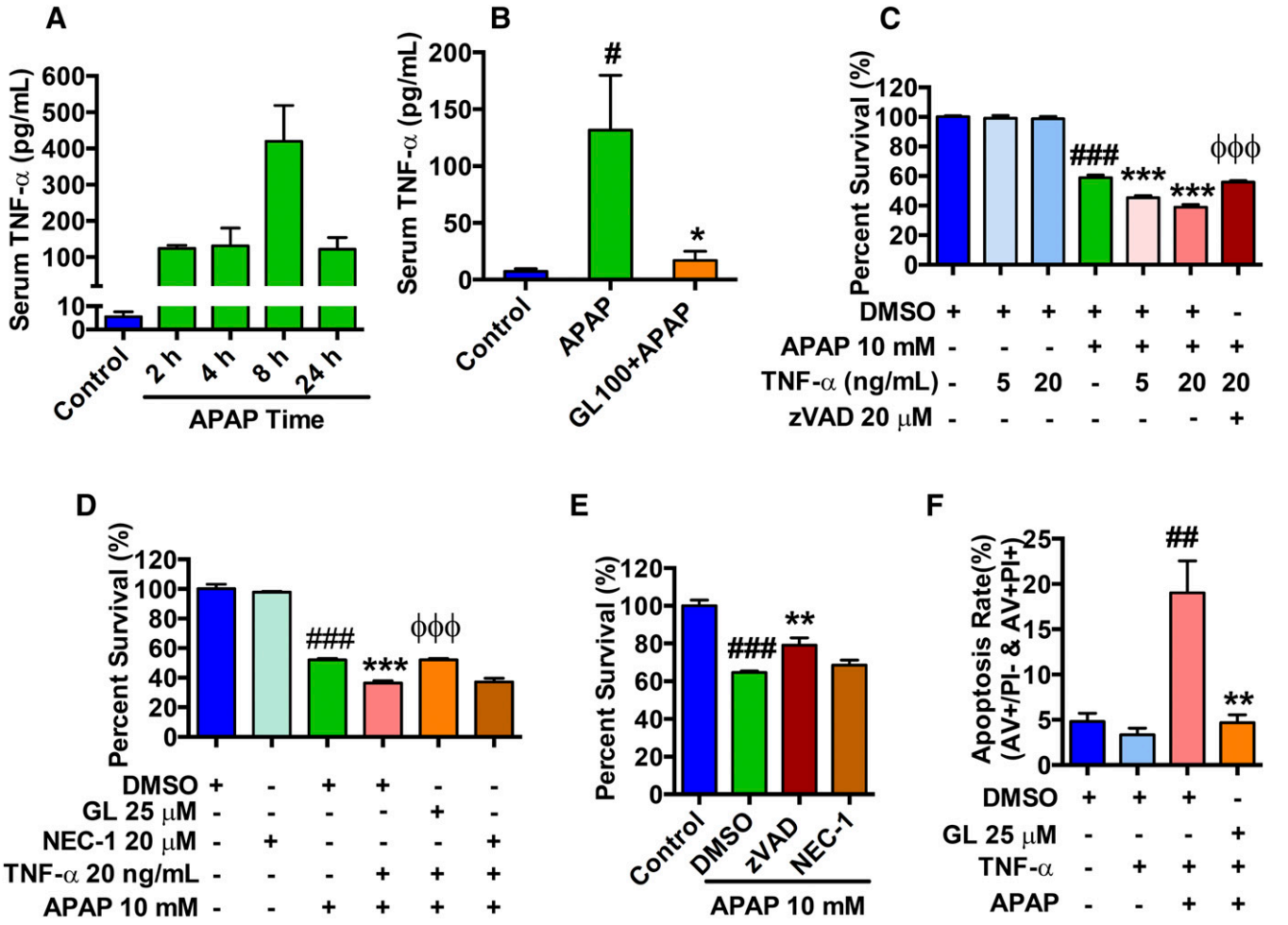

Fig. 10. GL attenuates APAP-caused TNFα release, and TNFα/caspase-mediated apoptotic hepatocyte damage. (A) Time course of APAP-induced TNFα release in serum. (B) Effect of GL in serum TNFα level at 4 hours after APAP treatment. (C) Effect of TNFα in APAP-induced LO2 cell death and effect of zVAD-fmk in TNFα/APAP-induced LO2 cell death. (D) Effects of GL and NEC-1 in TNFα/APAP-induced LO2 cell death. (E) Cell viability of APAP-treated LO2 cells pretreated with control DMSO, zVAD 20 μM, or NEC-1 20 μM. (F) Statistical analysis of FACS analyses. Number = 6 in each group for experiments in vivo in mice and in vitro in LO2 cells. Data are expressed as mean ± S.E.M. $^{\#}P < 0.05$, $^{\#\#}P < 0.01$, and $^{\#\#\#}P < 0.001$ versus control mice or 0.1% DMSO-treated control LO2 cells. $^{*}P < 0.05$, $^{**}P < 0.01$ and $^{***}P < 0.001$ versus APAP-overdosed mice or 0.1% DMSO/APAP-treated LO2 cells.$^{\phi\phi\phi}P < 0.001$ versus TNFα/APAP-treated LO2 cells.

fatty acids both in vivo and/or in vitro (Jeong et al., 2002; Gumpricht et al., 2005; Wu et al., 2008; Chen et al., 2013), GL and GA are considered to exert hepatoprotective effects by different mechanisms. Because formulations of GL for both intravenous and oral administration are available in the clinic (Li et al., 2014b), our data suggest that in the therapy of APAP-induced liver injury, intravenous, not oral, formulations of GL should be used.

CYP2E1-mediated activation of APAP is mainly responsible for initiating the cascade of APAP hepatotoxicity through formation of NAPQI (Lee et al., 1996). However, a single dose of GL alone did not change the CYP2E1 expression in our study and did not inhibit CYP2E1 activity in a previous study (Paolini et al., 1999). Conversely, GL significantly increased APAP-induced CYP2E1 down-regulation. The results in *Cyp2e1*-null mice further provide direct evidence that GL's protective effect is not dependent on CYP2E1 activity. Moreover, GL and GA have little effect on the metabolism of APAP and the enzymes involved in APAP metabolic activation. All these data strongly support that GL prevents APAP-induced liver injury independent of CYP2E1 and not through direct inhibition of APAP metabolic activation.

The role of RIPK3/necroptosis in APAP-induced toxicity is highly controversial (Ramachandran et al., 2013; Zhang et al., 2014). Another study suggested that RIPK3 was an early mediator in APAP toxicity and that RIPK3 protein, though absent at baseline, was induced in the liver at the early phase of APAP toxicity (An et al., 2013; Ramachandran et al., 2013; Zhang et al., 2014). *Ripk3*-null mice were reported to be protected at 6 hours after APAP overdosing, but the protective effect was lost at 24 hours after APAP challenge (Ramachandran et al., 2013). In our study, APAP also induced RIPK3 expression, at least at the mRNA level, which partially supports a previous study (Ramachandran et al., 2013). Unexpectedly, after further testing in *Ripk3*-null mice, no significant difference of sensitivity to APAP was found between *Ripk3*-null mice and their wild-type littermates, but GL markedly attenuated APAP-induced liver injury in both genotypes, suggesting no involvement of RIPK3 in APAP toxicity.

Our data on RIPK3/APAP toxicity are in agreement with a recent study that suggested no involvement of RIPK3 in mediating APAP toxicity (Dara et al., 2015). Our present work also revealed that APAP significantly induced *Mlkl* mRNA, a downstream target of RIPK3, and that GL did not decrease APAP-induced *Mlkl* mRNA up-regulation. Therefore, although RIPK3 up-regulation was observed upon APAP toxicity, it may not be an initiating factor in APAP toxicity.

The RIPK1 inhibitor NEC-1 was shown to inhibit APAP toxicity both in vivo and in primary hepatocytes in vitro (An et al., 2013; Ramachandran et al., 2013; Takemoto et al., 2014). In LO2 cells, both GL and the pan-caspase inhibitor zVAD, but not NEC-1, prevented APAP-induced cell death, suggesting that GL may act through a caspase-dependent apoptosis pathway, rather than via RIPK1/RIPK3-dependent necroptosis, in modulating APAP-induced hepatotoxicity.

Additional studies focused on elucidating how GL protected against apoptotic cell death of hepatocytes. TUNEL-positive staining and apoptotic hepatocyte death (which can be potentiated by TNFα) in vitro suggest the possible involvement of hepatic apoptosis in APAP toxicity. The previous reports on the involvement of apoptotic cell death in the APAP model have been controversial (Boulares et al., 2002; Matsumaru et al., 2003). It is widely believed that necrosis represents the exclusive cell death in APAP-overdosed livers with no detection of caspase activation (Jaeschke et al., 2006; Jaeschke et al., 2011). However, we found positive TUNEL staining at 2, 4, and 8 hours after APAP treatment, but the positive staining was sharply decreased at 24 hours. Because the necrotic areas were significantly increased across the time course, the transfer from apoptosis to late necrosis possibly explains the current observation (Possamai et al., 2013). Therefore, caspase-dependent apoptosis may be dominant in the early phase of APAP-induced hepatocyte death, which can be aggravated by APAP-induced release of TNFα, but may be rapidly transferred to typical necrosis or necroptosis through an unknown mechanism. Thus, GL may block caspase-dependent apoptotic cell death at the very early stage but not the latter necrotic phase of APAP toxicity.

TNF-deficient or TNF receptor type 1 (TNFR1)-deficient mice are not protected against APAP toxicity (Nagai et al., 2002; Chiu et al., 2003; James et al., 2005), indicating that TNFα/TNFR1 signaling is probably not an important factor in mediating APAP toxicity. However, TNFα, as a pleiotropic cytokine, can antagonize liver injury by facilitating liver regeneration, especially at low concentrations, and overrelease of TNF-α potentially aggravates hepatotoxicity. Thus, the results of TNF or TNFR1 knockout mice possibly represent an integrated effect of the two roles. The role of TNFα overrelease in aggravating APAP toxicity is still highly possible.

In our study, a direct role of TNFα in potentiating APAP-caused hepatocyte apoptosis in vitro was demonstrated in LO2 cells. These results agree with previous studies in primary hepatocytes (Colell et al., 1998; Matsumaru et al., 2003; Gandhi et al., 2010). GL shows a direct effect against TNFα/APAP-induced apoptotic cell death in LO2 cells, supporting that GL has a direct antiapoptotic effect. Of interest, APAP treatment induced an increase in the release of TNFα in serum, and GL repressed APAP-triggered release of TNFα. Therefore, the prevailing evidence suggests that APAP-induced TNFα overrelease at the very early phase of toxicity can potentially enhance APAP-induced hepatocyte death. Because GL is also an immunoregulator (Honda et al., 2012; Fu et al., 2014; Kim et al., 2015; Wu et al., 2015), it seems that GL could block both APAP-triggered TNFα release and its downstream apoptotic cascade.

In conclusion, the present study provides evidence that GL rather than its metabolite GA contributes to GL's protective effect in APAP-induced toxicity. GL's protective effect is independent of CYP2E1 and not through interference with APAP metabolic activation or RIPK3-mediated necroptosis. APAP-induced caspases-dependent apoptosis can be potentiated by TNFα and inhibited by GL. GL can suppress the APAP-induced inflammatory response and decrease TNFα release. Collectively, GL, not GA, potently prevents APAP toxicity through TNFα/caspase-mediated apoptotic cell death. Translationally, our study suggests that GL via intravenous injection but not oral intake is a potential option for clinical application. However, it is important to note that when GL was intravenously injected at 2 hours after APAP overdosing, when the liver was severely damaged, no significant hepatoprotective effect was observed in our study, although both multiple injections of GL and a single injection of GL showed a potent protective effect as a positive control (Supplemental Fig. 8, A and B). This suggests that GL alone may have limited clinical efficacy for combating APAP-induced liver injury. Farnesoid X receptor agonists could combat APAP toxicity via the promotion of liver regeneration, which is a latter phase of APAP toxicity (Xie et al., 2016). It would be of interest to determine whether the timely administration of GL in the early phase and farnesoid X receptor agonists in the latter phase would confer a synergy in combating APAP toxicity.

Acknowledgments

The authors thank Dr. Vishva Dixit (Genentech, Inc) for providing *Ripk3*-null mice.

Authorship Contributions

Participated in research design: Hao, G. Wang, Yan.

Conducted experiments: Yan, H. Wang, Zhao, Yagai, Chai, Krausz, Xie, Cheng, Zhang, Che, Li, Wu, Brocker.

Performed data analysis: Yan, Hao, H. Wang, Yagai.

Wrote or contributed to the writing of the manuscript: Yan, Yagai, Gonzalez, Hao, G. Wang.

References

Akao T, Hayashi T, Kobashi K, Kanaoka M, Kato H, Kobayashi M, Takeda S, and Oyama T (1994) Intestinal bacterial hydrolysis is indispensable to absorption of 18 beta-glycyrrhetic acid after oral administration of glycyrrhizin in rats. *J Pharm Pharmacol* **46**:135–137.

An J, Mehrhof F, Harms C, Lättig-Tünnemann G, Lee SLL, Endres M, Li M, Sellge G, Mandić AD, and Trautwein C, et al. (2013) ARC is a novel therapeutic approach against acetaminophen-induced hepatocellular necrosis. *J Hepatol* **58**:297–305.

Barakat W, Safwet N, El-Maraghy NN, and Zakaria MNM (2014) Candesartan and glycyrrhizin ameliorate ischemic brain damage through downregulation of the TLR signaling cascade. *Eur J Pharmacol* **724**:43–50.

Blieden M, Paramore LC, Shah D, and Ben-Joseph R (2014) A perspective on the epidemiology of acetaminophen exposure and toxicity in the United States. *Expert Rev Clin Pharmacol* **7**: 341–348.

Boulares AH, Zoltoski AJ, Stoica BA, Cuvillier O, and Smulson ME (2002) Acetaminophen induces a caspase-dependent and Bcl-XL sensitive apoptosis in human hepatoma cells and lymphocytes. *Pharmacol Toxicol* **90**:38–50.

Chan K, Hu XY, Razmovski-Naumovski V, and Robinson N (2015) Challenges and opportunities of integrating traditional Chinese medicine into mainstream medicine: a review of the current situation. *Eur J Integr Med* **7**:67–75.

Chen C, Krausz KW, Idle JR, and Gonzalez FJ (2008) Identification of novel toxicity-associated metabolites by metabolomics and mass isotopomer analysis of acetaminophen metabolism in wild-type and Cyp2e1-null mice. *J Biol Chem* **283**:4543–4559.

Chen S, Zou L, Li L, and Wu T (2013) The protective effect of glycyrrhetinic acid on carbon tetrachloride-induced chronic liver fibrosis in mice via upregulation of Nrf2. *PLoS One* **8**: e53662.

Cheung C, Yu AM, Ward JM, Krausz KW, Akiyama TE, Feigenbaum L, and Gonzalez FJ (2005) The cyp2e1-humanized transgenic mouse: role of cyp2e1 in acetaminophen hepatotoxicity. *Drug Metab Dispos* **33**:449–457.

Chiu H, Gardner CR, Dambach DM, Durham SK, Brittingham JA, Laskin JD, and Laskin DL (2003) Role of tumor necrosis factor receptor 1 (p55) in hepatocyte proliferation during acetaminophen-induced toxicity in mice. *Toxicol Appl Pharmacol* **193**:218–227.

Colell A, García-Ruiz C, Miranda M, Ardite E, Marí M, Morales A, Corrales F, Kaplowitz N, and Fernández-Checa JC (1998) Selective glutathione depletion of mitochondria by ethanol sensitizes hepatocytes to tumor necrosis factor. *Gastroenterology* **115**:1541–1551.

Dara L, Johnson H, Suda J, Win S, Gaarde W, Han D, and Kaplowitz N (2015) Receptor interacting protein kinase 1 mediates murine acetaminophen toxicity independent of the necrosome and not through necroptosis. *Hepatology* **62**:1847–1857.

Fan X, Jiang Y, Wang Y, Tan H, Zeng H, Wang Y, Chen P, Qu A, Gonzalez FJ, and Huang M, et al. (2014) Wuzhi tablet (*Schisandra sphenanthera* extract) protects against acetaminophen-induced hepatotoxicity by inhibition of CYP-mediated bioactivation and regulation of NRF2-ARE and p53/p21 pathways. *Drug Metab Dispos* **42**:1982–1990.

Fu Y, Zhou E, Wei Z, Song X, Liu Z, Wang T, Wang W, Zhang N, Liu G, and Yang Z (2014) Glycyrrhizin inhibits lipopolysaccharide-induced inflammatory response by reducing TLR4 recruitment into lipid rafts in RAW264.7 cells. *Biochim Biophys Acta* **1840**:1755–1764.

Gandhi A, Guo T, and Ghose R (2010) Role of c-Jun N-terminal kinase (JNK) in regulating tumor necrosis factor-alpha (TNF-alpha) mediated increase of acetaminophen (APAP) and chlorpromazine (CPZ) toxicity in murine hepatocytes. *J Toxicol Sci* **35**:163–173.

Gumpricht E, Dahl R, Devereaux MW, and Sokol RJ (2005) Licorice compounds glycyrrhizin and 18β-glycyrrhetinic acid are potent modulators of bile acid-induced cytotoxicity in rat hepatocytes. *J Biol Chem* **280**:10556–10563.

Hao H, Zheng X, and Wang G (2014) Insights into drug discovery from natural medicines using reverse pharmacokinetics. *Trends Pharmacol Sci* **35**:168–177.

Honda H, Nagai Y, Matsunaga T, Saitoh S, Akashi-Takamura S, Hayashi H, Fujii I, Miyake K, Muraguchi A, and Takatsu K (2012) Glycyrrhizin and isoliquiritigenin suppress the LPS sensor toll-like receptor 4/MD-2 complex signaling in a different manner. *J Leukoc Biol* **91**:967–976.

Jaeschke H, Cover C, and Bajt ML (2006) Role of caspases in acetaminophen-induced liver injury. *Life Sci* **78**:1670–1676.

Jaeschke H, Williams CD, and Farhood A (2011) No evidence for caspase-dependent apoptosis in acetaminophen hepatotoxicity. *Hepatology* **53**:718–719.

James LP, Kurten RC, Lamps LW, McCullough S, and Hinson JA (2005) Tumour necrosis factor receptor 1 and hepatocyte regeneration in acetaminophen toxicity: a kinetic study of proliferating cell nuclear antigen and cytokine expression. *Basic Clin Pharmacol Toxicol* **97**:8–14.

Jeong HG, You HJ, Park SJ, Moon AR, Chung YC, Kang SK, and Chun HK (2002) Hepatoprotective effects of 18beta-glycyrrhetinic acid on carbon tetrachloride-induced liver injury: inhibition of cytochrome P450 2E1 expression. *Pharmacol Res* **46**:221–227.

Jiang Y, Fan X, Wang Y, Chen P, Zeng H, Tan H, Gonzalez FJ, Huang M, and Bi H (2015) Schisandrol B protects against acetaminophen-induced hepatotoxicity by inhibition of CYP-mediated bioactivation and regulation of liver regeneration. *Toxicol Sci* **143**:107–115.

Kim YM, Kim HJ, and Chang KC (2015) Glycyrrhizin reduces HMGB1 secretion in lipopolysaccharide-activated RAW 264.7 cells and endotoxemic mice by p38/Nrf2-dependent induction of HO-1. *Int Immunopharmacol* **26**:112–118.

Lancaster EM, Hiatt JR, and Zarrinpar A (2015) Acetaminophen hepatotoxicity: an updated review. *Arch Toxicol* **89**:193–199.

Lawson JA, Farhood A, Hopper RD, Bajt ML, and Jaeschke H (2000) The hepatic inflammatory response after acetaminophen overdose: role of neutrophils. *Toxicol Sci* **54**:509–516.

Lee SS, Buters JT, Pineau T, Fernandez-Salguero P, and Gonzalez FJ (1996) Role of CYP2E1 in the hepatotoxicity of acetaminophen. *J Biol Chem* **271**:12063–12067.

Li FY, Hao HP, Hao K, Yan TT, and Wang GJ (2013) Effect of diammonium glycyrrhizinate on entecavir pharmacokinetics in rats. *Chin J Nat Med* **11**:309–313.

Li J, McQuade T, Siemer AB, Napetschnig J, Moriwaki K, Hsiao YS, Damko E, Moquin D, Walz T, and McDermott A, et al. (2012) The RIP1/RIP3 necrosome forms a functional amyloid signaling complex required for programmed necrosis. *Cell* **150**:339–350.

Li JX, Feng JM, Wang Y, Li XH, Chen XX, Su Y, Shen YY, Chen Y, Xiong B, and Yang CH, et al. (2014a) The B-Raf(V600E) inhibitor dabrafenib selectively inhibits RIP3 and alleviates acetaminophen-induced liver injury. *Cell Death Dis* **5**:e1278.

Li JY, Cao HY, Liu P, Cheng GH, and Sun MY (2014b) Glycyrrhizic acid in the treatment of liver diseases: literature review. *BioMed Res Int* **2014**:872139.

Liu ZX, Govindarajan S, and Kaplowitz N (2004) Innate immune system plays a critical role in determining the progression and severity of acetaminophen hepatotoxicity. *Gastroenterology* **127**:1760–1774.

Manyike PT, Kharasch ED, Kalhorn TF, and Slattery JT (2000) Contribution of CYP2E1 and CYP3A to acetaminophen reactive metabolite formation. *Clin Pharmacol Ther* **67**:275–282.

Matsumaru K, Ji C, and Kaplowitz N (2003) Mechanisms for sensitization to TNF-induced apoptosis by acute glutathione depletion in murine hepatocytes. *Hepatology* **37**:1425–1434.

McCarthy M (2014) FDA acts to limit exposure to acetaminophen in combination products. *BMJ* **348**:g356.

Mitka M (2014) FDA asks physicians to stop prescribing high-dose acetaminophen products. *JAMA* **311**:563.

Nagai H, Matsumaru K, Feng G, and Kaplowitz N (2002) Reduced glutathione depletion causes necrosis and sensitization to tumor necrosis factor-alpha-induced apoptosis in cultured mouse hepatocytes. *Hepatology* **36**:55–64.

Ni B, Cao Z, and Liu Y (2013) Glycyrrhizin protects spinal cord and reduces inflammation in spinal cord ischemia-reperfusion injury. *Int J Neurosci* **123**:745–751.

Paolini M, Barillari J, Broccoli M, Pozzetti L, Perocco P, and Cantelli-Forti G (1999) Effect of liquorice and glycyrrhizin on rat liver carcinogen metabolizing enzymes. *Cancer Lett* **145**: 35–42.

Possamai LA, McPhail MJW, Quaglia A, Zingarelli V, Abeles RD, Tidswell R, Puthucheary Z, Rawal J, Karvellas CJ, and Leslie EM, et al. (2013) Character and temporal evolution of apoptosis in acetaminophen-induced acute liver failure. *Crit Care Med* **41**:2543–2550.

Ramachandran A, McGill MR, Xie Y, Ni HM, Ding WX, and Jaeschke H (2013) Receptor interacting protein kinase 3 is a critical early mediator of acetaminophen-induced hepatocyte necrosis in mice. *Hepatology* **58**:2099–2108.

Sun L, Wang H, Wang Z, He S, Chen S, Liao D, Wang L, Yan J, Liu W, and Lei X, et al. (2012) Mixed lineage kinase domain-like protein mediates necrosis signaling downstream of RIP3 kinase. *Cell* **148**:213–227.

Takeda S, Ishthara K, Wakui Y, Amagaya S, Maruno M, Akao T, and Kobashi K (1996) Bioavailability study of glycyrrhetic acid after oral administration of glycyrrhizin in rats; relevance to the intestinal bacterial hydrolysis. *J Pharm Pharmacol* **48**:902–905.

Takemoto K, Hatano E, Iwaisako K, Takeiri M, Noma N, Ohmae S, Toriguchi K, Tanabe K, Tanaka H, and Seo S, et al. (2014) Necrostatin-1 protects against reactive oxygen species (ROS)-induced hepatotoxicity in acetaminophen-induced acute liver failure. *FEBS Open Bio* **4**: 777–787.

Wang X, Sun R, Wei H, and Tian Z (2013) High-mobility group box 1 (HMGB1)-Toll-like receptor (TLR)4-interleukin (IL)-23-IL-17A axis in drug-induced damage-associated lethal hepatitis: interaction of γδ T cells with macrophages. *Hepatology* **57**:373–384.

Wu CX, He LX, Guo H, Tian XX, Liu Q, and Sun H (2015) Inhibition effect of glycyrrhizin in lipopolysaccharide-induced high-mobility group box 1 releasing and expression from RAW264.7 cells. *Shock* **43**:412–421.

Wu X, Zhang L, Gurley E, Studer E, Shang J, Wang T, Wang C, Yan M, Jiang Z, and Hylemon PB, et al. (2008) Prevention of free fatty acid-induced hepatic lipotoxicity by 18β-glycyrrhetinic acid through lysosomal and mitochondrial pathways. *Hepatology* **47**:1905–1915.

Xie Y, Wang H, Cheng X, Wu Y, Cao L, Wu M, Xie W, Wang G, and Hao H (2016) Farnesoid X receptor activation promotes cell proliferation via PDK4-controlled metabolic reprogramming. *Sci Rep* **6**:18751.

Xiong X (2015) Integrating traditional Chinese medicine into Western cardiovascular medicine: an evidence-based approach. *Nat Rev Cardiol* **12**:374.

Yu J, Jiang YS, Jiang Y, Peng YF, Sun Z, Dai XN, Cao QT, Sun YM, Han JC, and Gao YJ (2014) Targeted metabolomic study indicating glycyrrhizin's protection against acetaminophen-induced liver damage through reversing fatty acid metabolism. *Phytother Res* **28**:933–936.

Zhang DW, Shao J, Lin J, Zhang N, Lu BJ, Lin SC, Dong MQ, and Han J (2009) RIP3, an energy metabolism regulator that switches TNF-induced cell death from apoptosis to necrosis. *Science* **325**:332–336.

Zhang L and Schuppan D (2014) Traditional chinese medicine (TCM) for fibrotic liver disease: hope and hype. *J Hepatol* **61**:166–168.

Zhang YF, He W, Zhang C, Liu XJ, Lu Y, Wang H, Zhang ZH, Chen X, and Xu DX (2014) Role of receptor interacting protein (RIP)1 on apoptosis-inducing factor-mediated necroptosis during acetaminophen-evoked acute liver failure in mice. *Toxicol Lett* **225**:445–453.

Zhao J, Jitkaew S, Cai Z, Choksi S, Li Q, Luo J, and Liu ZG (2012) Mixed lineage kinase domain-like is a key receptor interacting protein 3 downstream component of TNF-induced necrosis. *Proc Natl Acad Sci USA* **109**:5322–5327.

Zheng X, Zhang X, Wang G, and Hao H (2015) Treat the brain and treat the periphery: toward a holistic approach to major depressive disorder. *Drug Discov Today* **20**:562–568.

Address correspondence to: Dr. Guangji Wang, State Key Laboratory of Natural Medicines, Key Laboratory of Drug Metabolism and Pharmacokinetics, China Pharmaceutical University, No. 24, Tongjiaxiang, Nanjing 210009, People's Republic of China. E-mail: guangjiwang@hotmail.com or Dr. Haiping Hao, State Key Laboratory of Natural Medicines, Key Laboratory of Drug Metabolism and Pharmacokinetics, China Pharmaceutical University, No. 24, Tongjiaxiang, Nanjing 210009, People's Republic of China. E-mail: haipinghao@cpu.edu.cn